A Novel Fluorescent Ceramide Analogue for Studying Membrane Traffic in Animal Cells: Accumulation at the Golgi Apparatus Results in Altered Spectral Properties of the Sphingolipid Precursor

Richard E. Pagano,* Ona C. Martin,* Hee Chol Kang,‡ and Richard P. Haugland‡

*Department of Embryology, Carnegie Institution of Washington, Baltimore, Maryland 21210; and
‡Molecular Probes, Inc., Eugene, Oregon 97402

Abstract. A series of ceramide analogues bearing the fluorophore boron dipyrromethene difluoride (BODIPY) were synthesized and evaluated as vital stains for the Golgi apparatus, and as tools for studying lipid traffic between the Golgi apparatus and the plasma membrane of living cells. Studies of the spectral properties of several of the BODIPY-labeled ceramides in lipid vesicles demonstrated that the fluorescence emission maxima were strongly dependent upon the molar density of the probes in the membrane. This was especially evident using *N*-[5-(5,7-dimethyl BODIPY)-1-pentanoyl]-D-*erythro*-sphingosine (C_5-DMB-Cer), which exhibited a shift in its emission maximum from green (~515 nm) to red (~620 nm) wavelengths with increasing concentrations. When C_5-DMB-Cer was used to label living cells, this property allowed us to differentiate membranes containing high concentrations of the fluorescent lipid and its metabolites (the corresponding analogues of sphingomyelin and glucosylceramide) from other regions of the cell where smaller amounts of the probe were present. Using this approach, prominent red fluorescent labeling of the Golgi apparatus, Golgi apparatus–associated tubulovesicular processes, and putative Golgi apparatus transport vesicles was seen in living human skin fibroblasts, as well as in other cell types. Based on fluorescence ratio imaging microscopy, we estimate that C_5-DMB-Cer and its metabolites were present in Golgi apparatus membranes at concentrations up to 5–10 mol %. In addition, the concentration-dependent spectral properties of C_5-DMB-Cer were used to monitor the transport of C_5-DMB-lipids to the cell surface at 37°C.

STUDIES of lipid traffic at the Golgi complex have been made possible in recent years using a fluorescent analogue of ceramide (Cer)[1], *N*-[7-(4-nitrobenzo-2-oxa-1,3-diazole)]-6-aminocaproyl-D-*erythro*-sphingosine (C_6-NBD-Cer) (reviewed in 30). This molecule is a vital stain for the Golgi apparatus (24), and, in combination with fluorescence video imaging, has been used to study the dynamics of this organelle within living cells (8). C_6-NBD-Cer also stains the Golgi apparatus of fixed cells, most likely through interaction(s) with endogenous lipids and cholesterol, and serves as a *trans*-Golgi marker for both light and electron microscopy in these preparations (29, 33). Similar to its endogenous counterpart, C_6-NBD-Cer is metabolized in living cells to sphingomyelin (SM) and a glycolipid, glucosylceramide (GlcCer) (17, 22, 23, 32, 44, 45). These fluorescent metabolites are subsequently transported to the plasma membrane of cells from the Golgi complex by a vesicle-mediated process (17, 23). In polarized cells the fluorescent Cer is metabolized to fluorescent analogues of SM and GlcCer, and the latter is preferentially delivered to the apical cell surface (44, 45). This polarized delivery is consistent with the known enrichment of glycosphingolipids in apical membranes, and indicates that C_6-NBD-Cer and its metabolites are recognized by the cellular sorting and transport machinery in a manner similar to their natural counterparts.

Although much useful information has already been obtained using C_6-NBD-Cer, there are several disadvantages of this probe. First, the NBD-fluorophore is rapidly bleached during observation under a conventional fluorescence microscope. As a result, samples are usually focused during brief exposure to attenuated light before photography, and repeated observation and photography of a single cell is virtually impossible without low light level imaging equipment. Second, although C_6-NBD-Cer vitally stains the Golgi apparatus of

1. *Abbreviations used in this paper*: BODIPY, boron dipyrromethene difluoride; C_5-DMB-, *N*-[5-(5,7-dimethyl BODIPY)-1-pentanoyl]; C_5-DMB-Cer, *N*-[5-(5,7-dimethyl BODIPY)-1-pentanoyl]-D-*erythro*-sphingosine; C_5-DMB-SM, *N*-[5-(5,7-dimethyl BODIPY)-1-pentanoyl]-sphingosylphosphorylcholine; C_6-NBD-Cer, *N*-[7-(4-nitrobenzo-2-oxa-1,3-diazole)]-6-aminocaproyl-D-*erythro*-sphingosine; Cer, ceramide; DF-BSA, defatted BSA; GlcCer, glucosylceramide; HMEMB, 10 mM 4-(2-hydroxyethyl)-1-piperazineethane sulfonic acid-buffered MEM, pH 7.4, without indicator, and containing 0.5 mM each choline chloride, ethanolamine, serine, and (myo) inositol; POPC, 1-palmitoyl, 2-oleoyl phosphatidylcholine; SM, sphingomyelin.

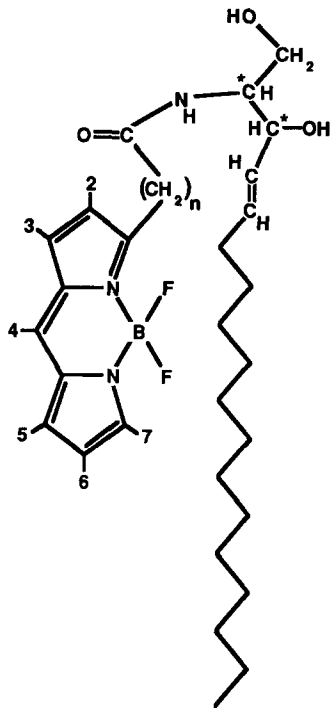

Figure 1. Generalized structure of a BODIPY-labeled ceramide analogue. In the case of C_5-DMB-Cer, $n = 4$, and methyl groups are present at positions 5 and 7 of the BODIPY moiety. Asterisks denote chiral carbon atoms on the sphingosine backbone. In the current study only D-*erythro*-sphingosine (2S, 3R) was used.

cells, prominent labeling of other intracellular membranes (e.g., the ER, mitochondria, and nuclear envelope) also occurs. Thus, some features of Golgi apparatus morphology may be obscured by fluorescence present in adjacent areas of the cells. Finally, biophysical studies of NBD-labeled lipids in model membrane systems indicate that although the NBD-fluorophore is attached to the acyl chain of the lipid, it is not fully intercalated in the membrane bilayer, but rather "loops up" to the membrane/water interface because of its polar nature (6, 7; Wolf, D. E., A. Winiski, A. E. Ting, K. M. Bocian, and R. E. Pagano, manuscript submitted for publication). Although this phenomenon does not appear to inhibit the metabolism of C_6-NBD-Cer or the intracellular sorting and transport of its metabolites, it may limit as yet unknown metabolic and/or transport processes in which the analogue can participate.

In the present study we describe a new fluorescent Cer analogue that overcomes some of the problems cited above. This analogue is a conjugate of D-*erythro*-sphingosine and a fluorescent fatty acid containing the fluorophore boron dipyrromethene difluoride (BODIPY) (Fig. 1). The BODIPY fluorophore has an approximately two- to threefold higher fluorescence yield and greater photostability than NBD (Johnson, I. D., H. C. Kang, and R. P. Haugland, unpublished observations). The BODIPY Cer analogue presented in this study is also of particular interest because its fluorescence emission spectrum is dramatically red-shifted as the probe concentrates at the Golgi apparatus. Thus, with the appropriate microscope filters, the Golgi apparatus can be observed within living cells without interfering fluorescence from other intracellular membranes.

Materials and Methods

Cells and Cell Culture

Normal (GM 5659) human skin fibroblasts were obtained from the Coriell Institute, Human Genetic Mutant Cell Repository (Camden, NJ). The cells were grown in MEM supplemented with 10% FBS, 2 mM L-glutamine, 100 U/ml penicillin, 100 μg/ml streptomycin, and 0.1 mM each nonessential amino acids. Swiss 3T3 cells (CCL 92) were obtained from the American Type Culture Collection (Rockville, MD) and grown as described (41). BHK-21 fibroblasts (American Type Culture Collection, CCL10) were grown in Dulbecco's MEM supplemented with 10% FBS, 2 mM L-glutamine, 100 U/ml penicillin, and 100 μg/ml streptomycin. 4-d-old chick skeletal muscle cell cultures, generously supplied by Dr. Douglas Fambrough (The Johns Hopkins University), were prepared as described (9) and grown in Eagle's MEM supplemented with 2% chick embryo extract and 10% horse serum. Liquid MEM was from Biofluids, Inc. (Rockville, MD), FBS was from HyClone Laboratories, Inc. (Logan, UT), and all other supplements were from Gibco Laboratories (Grand Island, NY).

For fluorescence microscopy, cells were grown on no. 1 thickness glass coverslips. For biochemical studies, GM 5659 cells were grown in 60- or 100-mm diameter tissue culture dishes. All cells were grown at 37°C in a water-saturated atmosphere of 5% CO_2 in air.

Lipids

1-Palmitoyl, 2-oleoyl phosphatidylcholine (POPC) was purchased from Avanti Biochemicals, Inc. (Pelham, AL). C_6-NBD-Cer was synthesized and purified as described (32). An intact Golgi apparatus fraction was prepared from rat liver homogenates as described (2, 11), and the lipids were extracted using the method of Bligh and Dyer (3). The phospholipid concentration in the extract was then determined (35), however, this was an underestimate of the total lipid concentration since nonphosphorus-containing lipids were also present.

N-[5-(5,7-dimethyl BODIPY)-1-pentanoyl]-D-erythro-sphingosine (C_5-DMB-Cer), -sphingosylphosphorylcholine (C_5-DMB-SM), and -glucosylsphingosine (C_5-DMB-GlcCer) were prepared by *N*-acylation (38) of D-*erythro*-sphingosine, sphingosylphosphorylcholine, and glucosylsphingosine, respectively, using the *N*-hydroxysuccinimide ester of 5-(5,7-dimethyl BODIPY)-1-pentanoic acid (Molecular Probes, Inc., Eugene, OR). The resulting fluorescent analogues of Cer, SM, and GlcCer were purified by preparative TLC. The structure of C_5-DMB-Cer was confirmed by ^1H NMR spectroscopy.

Concentrations of lipid stock solutions were determined by phosphorus measurement (35) or by reference to known concentrations of fluorescent standards.

Fluorescent Lipid/BSA Complexes and Lipid Vesicles

A complex of C_5-DMB-Cer with defatted BSA (DF-BSA) was prepared as described (32). The complex was ~5 μM in both the fluorescent lipid and DF-BSA and was prepared in 10 mM 4-(2-hydroxyethyl)-1-piperazineethane sulfonic acid-buffered Eagle's MEM, pH 7.4, without indicator, and containing 0.5 mM each choline chloride, ethanolamine, serine, and (myo) inositol (HMEMB).

Small unilamellar lipid vesicles were prepared by ethanol injection (20) using various amounts of C_5-DMB-Cer (or C_5-DMB-SM) and either POPC or rat liver Golgi membrane lipids. For calibration of fluorescence ratio images (see below), large unilamellar vesicles containing POPC and various amounts of C_5-DMB-Cer were prepared by extrusion through 0.1 μm polycarbonate filters (12). All vesicle preparations were made in 10 mM Hepes-buffered Ca- and Mg-free Puck's saline, pH 7.4.

Incubation of Fluorescent Lipids with Cells

Cultures were washed in HMEMB, incubated with 5 μM C_5-DMB-Cer/DF-BSA in HMEMB for 30 min at 2°C, washed, and further incubated in HMEMB for various times at 37°C before observation and photography or lipid extraction and analysis (see below). In some experiments, fluorescent lipid-treated cells were fixed for 10–15 min at 22°C in 0.5% glutaraldehyde and washed before observation and photography.

Lipid Analysis

Cells were harvested for lipid extraction using a rubber policeman and then extracted by the procedure of Bligh and Dyer (3), using 0.9% NaCl and 10 mM HCl in the aqueous phase. Lipid extracts were analyzed qualitatively by TLC using $CHCl_3/CH_3OH$/15 mM $CaCl_2$ (60:35:8, vol/vol/vol) as the developing solvent and quantified as described (18).

Fluorescence Microscopy

Fluorescence microscopy was performed with an inverted microscope (IM-

35; Carl Zeiss, Inc., Thornwood, NY) equipped with a Planapo 100× (1.3 NA) objective and epifluorescence optics (see Table I). Black and white photomicrographs were obtained using Tri-X film (Eastman Kodak Co., Rochester, NY) and processed at ASA 1600 with Diafine developer (Acufine, Inc., Chicago, IL). Color photomicrographs were obtained using Kodachrome 200 film which was processed by Kodak Film Laboratories (Rockville, MD).

Fluorescence ratio imaging microscopy (4, 5) was performed using a Universal microscope (Carl Zeiss, Inc.) equipped with a 63× (1.4 NA) Planapo objective and epifluorescence optics. Samples were excited with blue light and observations were made in the "green" and "red" regions of the spectrum (see Table I). A KS-1380 image intensifier (Videoscope International, Ltd., Washington, DC) coupled to a video camera (CCD-71; Dage-MTI, Inc., Michigan City, IN) was used to obtain images through the microscope. Both cameras were operated at medium gain and in the linear portion of their sensitivity ranges. To minimize photobleaching, samples were briefly illuminated with attenuated light for focusing purposes and during image collection (~1 s/exposure). 32 fluorescence video images of C_5-DMB-Cer-treated cells were digitized and averaged using an Image 1/AT Image Processing System (Universal Imaging Corp., Media, PA). Images in the green and red channels of blank areas of the culture dish were also obtained and used for background subtraction. For calibration purposes (see Fig. 5), lipid vesicles formed from POPC and various amounts of C_5-DMB-Cer were used; background images were obtained using POPC vesicles containing no C_5-DMB-Cer.

EM Studies of C_5-DMB-Cer in Cells

The distribution of C_5-DMB-Cer at the EM level was determined as described (33) with several modifications. Briefly, cells grown on 35-mm diameter tissue culture dishes were incubated with 5 μM C_5-DMB-Cer/DF-BSA for 30 min at 2°C, washed, and further incubated for 30 min at 37°C in HMEMB. The cells were then fixed in 1% glutaraldehyde/0.1 M cacodylate buffer (pH 7.4) for 30 min at 22°C. The samples were then washed in 0.1 M Tris buffer (pH 7.6) and 0.9 ml of a fresh solution of 1.5 mg 3,3'-DAB tetrahydrochloride (Polysciences, Inc., Warrington, PA) per ml 0.1 M Tris buffer (pH 7.6) was added to the culture dish. After 10 min, an area of the culture dish was irradiated for 30 min at 22°C using the 476.5-nm line of a tunable argon laser operating at 50 mW power. To obtain a relatively large area of irradiated cells, the laser beam was expanded to a line ~1 mm wide by 1 cm long using a cylindrical lens. After irradiation, the sample was washed in 0.1 M Tris buffer (pH 7.6), rinsed in 0.1 M cacodylate buffer (pH 7.4), and treated with 1% OsO_4 in 0.1 M cacodylate buffer for 60 min at 22°C. The sample was then washed in 0.1 M cacodylate buffer and processed for EM as described (33). Control samples were treated as described above, except that incubation with C_5-DMB-Cer was omitted. Thin EPON sections were obtained with a Porter-Blum MT-2 ultramicrotome (DuPont Instruments, Sorvall Operations, Newton, CT), mounted on Formvar-coated grids, and stained with lead citrate before examination. Electron micrographs were obtained with a JEOL 100S electron microscope operating at 80 kV.

Other Chemicals and Procedures

Unless otherwise noted, all other chemicals were purchased from Sigma Chemical Co. (St. Louis, MO). Fluorescence spectra were obtained using an SLM-8000C spectrophotofluorimeter.

Results

C_5-DMB-Cer in Lipid Vesicles

The fluorescence emission spectra of lipid vesicles comprised of POPC and various amounts of C_5-DMB-Cer are shown in Fig. 2. At low mole fractions, a single fluorescence emission peak at ~515 nm was observed. However, with increasing mole fractions this fluorescence decreased in intensity while a second peak of fluorescence appeared at ~620 nm. The ratio of fluorescence intensities at 620 and 515 nm increased linearly from 2 to 50 mol % C_5-DMB-Cer (Fig. 2, *inset*), and this ratiometric data was independent of polarization (data not shown). Virtually identical results were obtained using POPC vesicles containing C_5-DMB-SM in place of C_5-DMB-Cer (data not shown), demonstrating that the shift in fluorescence emission was not limited to the Cer analogue. In addition, identical spectral shifts were obtained when C_5-DMB-Cer was incorporated into lipid vesicles prepared from POPC or from lipids extracted from rat liver

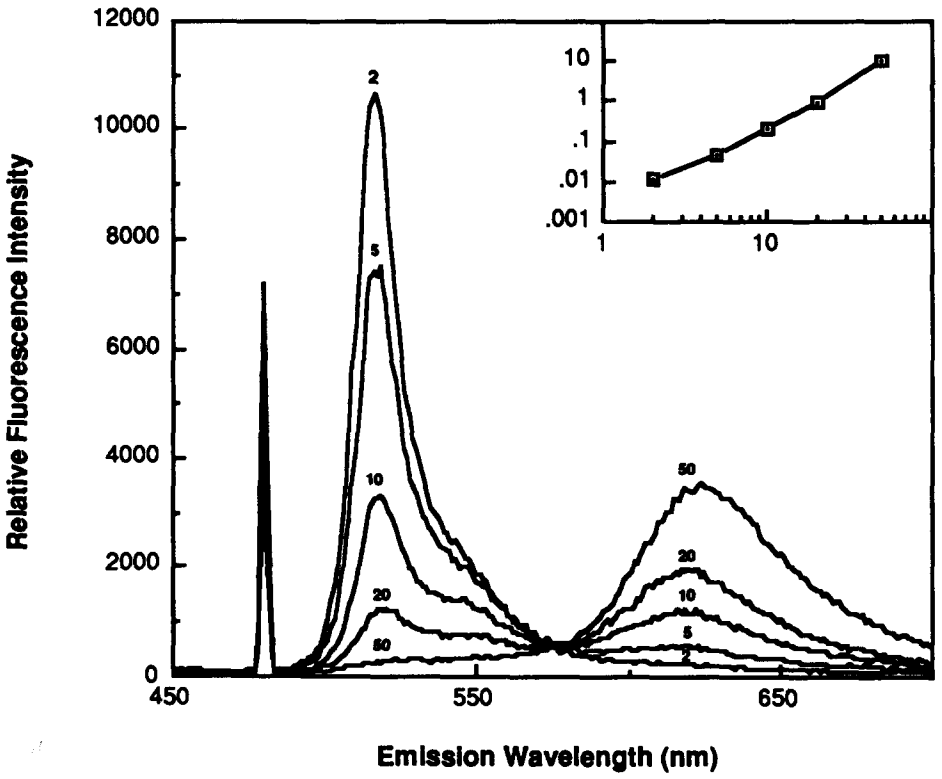

Figure 2. Fluorescence emission spectra of lipid vesicles containing various amounts of C_5-DMB-Cer. Emission spectra of small unilamellar vesicles formed from POPC and 2, 5, 10, 20, or 50 mol % C_5-DMB-Cer (total lipid concentration was 31 μM). Excitation was at 480 nm. (*inset*) Ratio of relative fluorescence intensities at 620 and 515 nm vs mol % C_5-DMB-Cer. Data for inset were obtained using excitation and emission polarizers positioned at 54.7°.

Table I. Optical Filters for Microscopy of C_5-DMB-Lipids

Channel	Zeiss filter pack components			Spectral window	
	Exciter filter	Dichroic beam splitter	Barrier filter	Excitation wavelength	Emission wavelength
Green	BP450-490	FT510	BP520-560	450–490	520–560
Green + Red	BP450-490	FT510	LP520	450–490	⩾520
Red	BP450-490	FT510	LP590	450–490	⩾590

Golgi apparatus membranes (data not shown), suggesting that the shift in fluorescence emission was not dependent on the presence of POPC. However, we did not make a quantitative comparison of the fluorescence intensities at 620 and 515 nm, because the total amount of lipid present in the rat liver Golgi extracts was unknown (see Materials and Methods).

C_5-DMB-Cer Distribution and Metabolism in Living Cells

Table I summarizes the optical filters used for examining specimens treated with C_5-DMB-Cer. These filters established three spectral windows or "channels" which excited the specimens with blue light (450–490 nm), and allowed visualization of fluorescence in the green (520–560 nm), green + red (⩾520 nm), or red (⩾590 nm) regions of the spectrum.

Typical fluorescence micrographs of human skin fibroblasts treated with C_5-DMB-Cer are shown in Fig. 3. When cells were observed in the green + red channel, a bright perinuclear and reticular pattern of fluorescence corresponding to the Golgi apparatus (see below) was seen. The fluorescence at the Golgi apparatus was yellow/orange in color and was in striking contrast to the weaker green fluorescence which was seen in other intracellular membranes. By reference to previous studies with C_6-NBD-Cer (22, 23), these other membranes most likely corresponded to the ER, mitochondria, and nuclear envelope. Some labeling of the plasma membrane was also visible under these incubation conditions. When the same cells were observed in the red channel, the Golgi apparatus was brilliantly fluorescent, but little or no fluorescence was detected in other intracellular membranes. No change in the distribution of fluorescence was observed when C_5-DMB-Cer–treated cells were fixed in 0.5% glutaraldehyde (10–15 min at 22°C) and then observed under the fluorescence microscope (data not shown).

The presence of C_5-DMB-Cer at the Golgi apparatus was confirmed using a previously described method for visualizing C_6-NBD-Cer at the EM level (33). This method is based on the photoconversion of a fluorescent marker to a DAB product (26, 36). Human skin fibroblasts treated with C_5-DMB-Cer showed significant amounts of the osmiophilic DAB polymer at the Golgi apparatus and in Golgi-associated vesicles (Fig. 4). No DAB polymer was seen in control experiments in which C_5-DMB-Cer was omitted from the specimen, or in C_5-DMB-Cer–treated cells that were not irradiated. As previously seen for C_6-NBD-Cer (33), C_5-DMB-Cer labeled only a subset of Golgi stacks.

We estimated the amount of C_5-DMB-lipid present at the Golgi apparatus of treated cells by fluorescence ratio imaging microscopy (4, 5). Fluorescence images of single cells (see Materials and Methods) were first obtained using the green and red microscope channels (see Table I), and, after background subtraction, the ratio of the two images was calculated and displayed as a spatial map in pseudocolor. A typical result is shown in Fig. 5 *a*, in which it was readily apparent that the ratio of red to green fluorescence was greatest at the Golgi apparatus. To relate this fluorescence ratio image to the concentration of C_5-DMB-lipids present at the Golgi apparatus, a standard curve was derived using lipid vesicles containing various amounts of C_5-DMB-Cer (Fig. 5 *b*). Similar to the results shown in Fig. 2 (*inset*), we found that fluorescence ratio imaging measurements resulted in a plot in which the ratio was linear with respect to the concentration of C_5-DMB-Cer (Fig. 5 *b*). Using this calibration curve and data obtained from different preparations of cells ($n = 57$) we calculated that the maximum concentration of C_5-DMB-Cer at the Golgi apparatus ranged from 5 to 10 mol %. In control experiments we found that the ratio images of C_5-DMB-Cer–treated cells were unaffected by the order in which the green and red images were obtained (data not shown).

Fig. 6 shows the distribution of fluorescence in cells that were incubated with C_5-DMB-Cer at 2°C, washed, and warmed to 37°C for 0–120 min. When cells were observed in the green + red channel, intracellular fluorescence was seen at all time points and only subtle changes in distribution were detected. Although no Golgi apparatus labeling was seen immediately after incubation with C_5-DMB-Cer at 2°C (Fig. 6 *a*), such labeling was readily seen at all subsequent time points (Fig. 6, *b–f*). In contrast, dramatic changes in the distribution of red channel fluorescence were seen with time at 37°C. Immediately after incubation with C_5-DMB-Cer at 2°C, weak fluorescence was detected at the plasma membrane of cells (Fig. 6 *a*). After 5 min at 37°C, plasma membrane labeling was no longer apparent, but, in some cells, weak labeling of the Golgi apparatus was detected (Fig. 6 *b*). After 15 min, bright labeling of the Golgi apparatus, but not other intracellular membranes, was readily apparent (Fig. 6 *c*). After 30 min at 37°C, small spots of fluorescence scattered throughout the cytoplasm (Fig. 6 *d*, *arrows*) could be seen in addition to prominent labeling of the Golgi apparatus. A similar pattern of fluorescence was seen at later times, except that by 60 min, some plasma membrane labeling was also detected (Fig. 6 *e*). Labeling of the plasma membrane increased somewhat with further incubation at 37°C (Fig. 6 *f*). Interestingly, no changes in the apparent intensity of Golgi apparatus labeling were seen between 15 and 120 min at 37°C.

We also examined the effect of temperature on the redistribution of C_5-DMB-fluorescence (Fig. 7). In these experiments, cells were incubated with C_5-DMB-Cer for 30 min

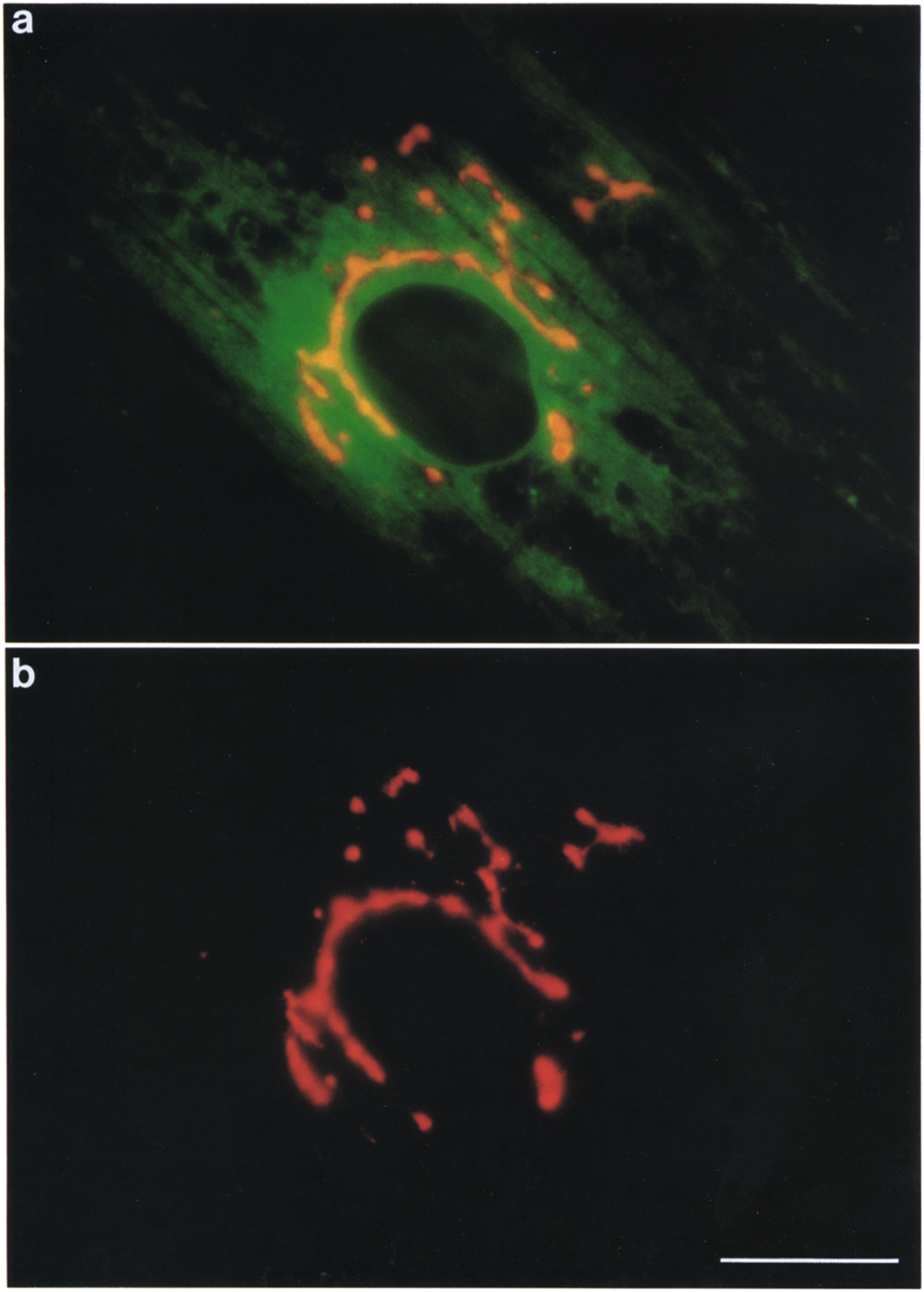

Figure 3. Fluorescence micrographs of human skin fibroblasts after incubation with C_5-DMB-Cer. Cells were incubated with 5 μM C_5-DMB-Cer/DF-BSA for 30 min at 2°C, washed, further incubated for 30 min at 37°C in HMEMB, and photographed in the (*a*) green + red and (*b*) red microscope channels (see Table I). Bar, 20 μm.

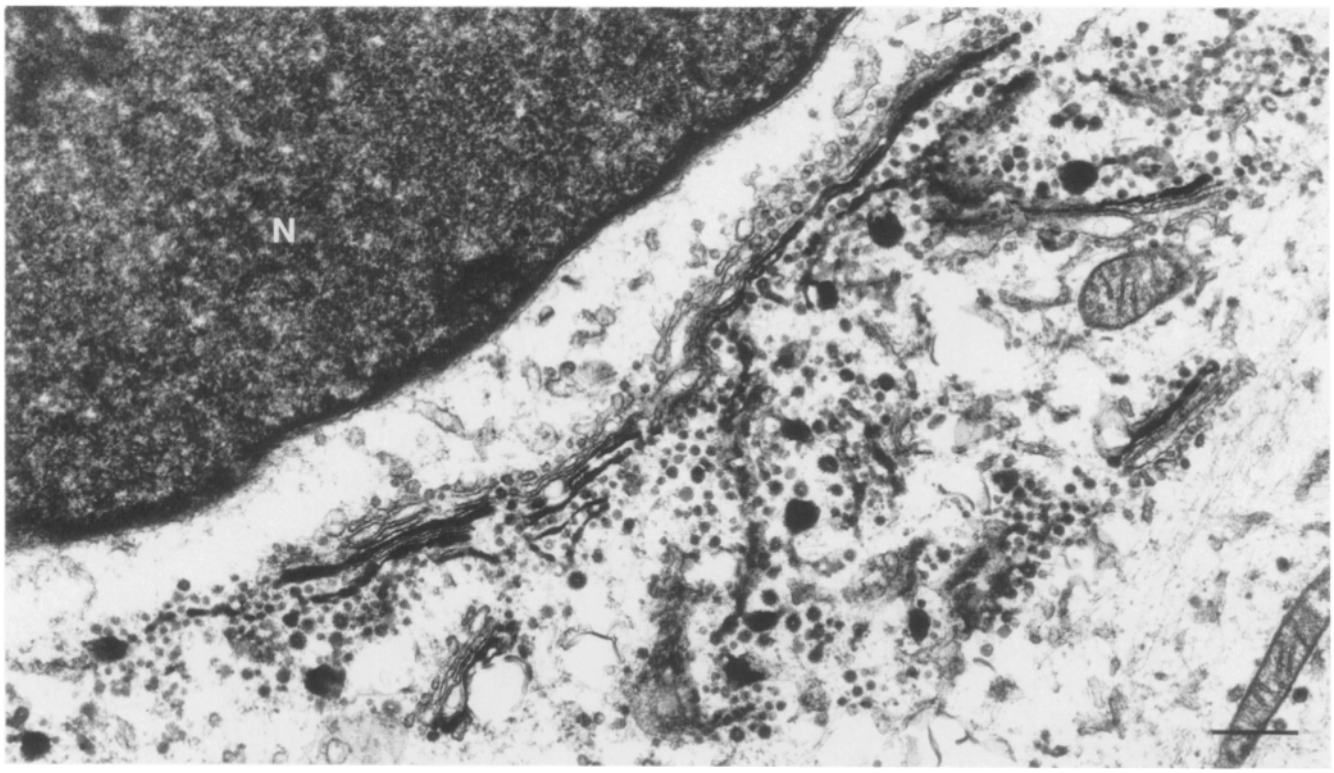

Figure 4. EM localization of C_5-DMB-Cer at the Golgi apparatus of human skin fibroblasts. Cells were incubated with C_5-DMB-Cer as in Fig. 3, fixed, photobleached in the presence of DAB, washed, and processed for EM (see Materials and Methods). Note that numerous vesicles near the Golgi cisternae, as well as some Golgi stacks, were labeled by this procedure. *N*, nucleus. Bar, 0.5 μm.

at 2°C, washed, warmed to 37°C for 30 min, and then further incubated at either 20°C (Fig. 7 *a*) or 37°C (Fig. 7 *b*). Little plasma membrane labeling was seen after the 20°C incubation. Also, in some cells, prominent microprojections or "spikes" from the Golgi apparatus were seen. These were most apparent when specimens were warmed for 30 min at 37°C and then incubated at 22°C for ≥60 min (Fig. 7 *c*). These extensive processes appeared to be identical to the tubulovesicular processes extending from the Golgi apparatus which have recently been observed at the light microscope level in other cell types (8, 21).

Biochemical studies established that C_5-DMB-Cer was metabolized at 37°C to two new fluorescent lipids (Fig. 8) which were identified as the corresponding fluorescent analogues of -SM and -GlcCer by TLC and reference to authentic standards of these lipids.

Comparison of C_5-DMB-Cer and C_6-NBD-Cer in Different Cell Types

We compared the patterns of intracellular fluorescence obtained after treatment of various cell types with C_5-DMB-Cer or C_6-NBD-Cer (Fig. 9). Cells treated with either analogue and observed in the green channel showed similar patterns of intracellular fluorescence in which labeling of the Golgi apparatus, ER, nuclear envelope, and mitochondria were seen. In contrast, each cell type showed prominent and more specific labeling of the Golgi apparatus after treatment with C_5-DMB-Cer and observation in the red channel.

Other BODIPY Cer Analogues

We also examined the spectral properties of several other BODIPY Cer analogues and their intracellular distribution and metabolism in human skin fibroblasts (data not shown). These analogues all had the same general structure shown in Fig. 1, however, the chain length of the fatty acid and the number and type of substituents on the BODIPY ring were varied. Each of the analogues labeled the Golgi apparatus of cells and each was metabolized to the corresponding fluorescent analogue of SM, but little if any metabolism to GlcCer was seen. Although a number of the BODIPY Cer analogues showed significant "red shifts" in fluorescence, C_5-DMB-Cer was used in the present study because the shift was large (~100 nm) and the two peaks of fluorescence could be visualized separately under a conventional fluorescence microscope using standard microscope filters.

Discussion

In this study we examined a series of fluorescent (BODIPY) Cer analogues as possible alternative probes to C_6-NBD-Cer for studying lipid traffic at the Golgi apparatus and the dynamics of this organelle in situ. These analogues were synthesized and tested as alternative probes because (*a*) the BODIPY fluorophore has a significantly higher fluorescence yield and greater photostability than NBD; (*b*) the emission properties of BODIPY can be shifted by the addition of various substituents on the parent compound (data not shown);

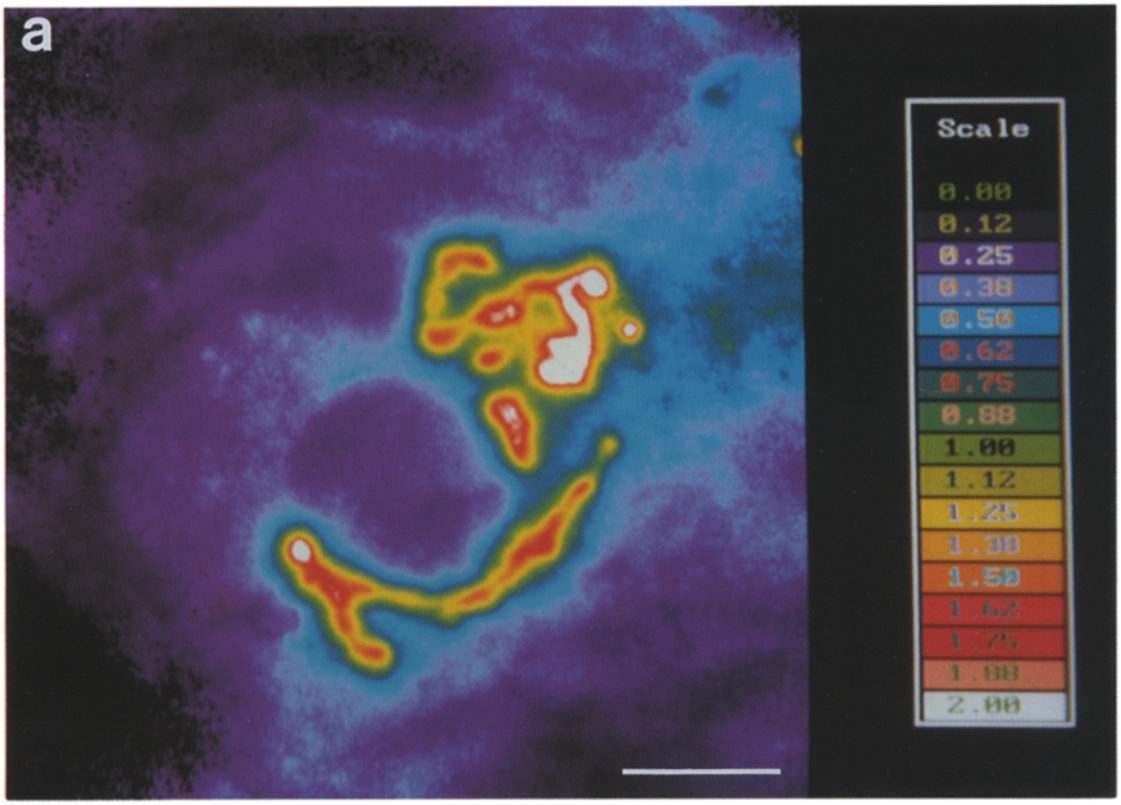

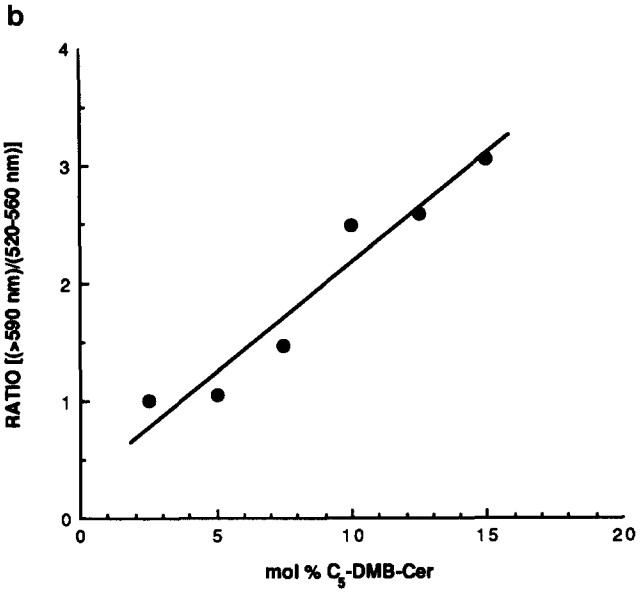

Figure 5. Fluorescence ratio imaging microscopy of C_5-DMB-Cer–treated cells and of lipid vesicles. (*a*) Human skin fibroblasts were incubated with C_5-DMB-Cer as in Fig. 3. Images in the red and green microscope channels (Table I) were then obtained, and, after background subtraction, the ratio was calculated and displayed as a pseudocolor image. The scale on the right relates the calculated ratio to the color displayed. (*b*) Ratio of red to green fluorescence vs mol % C_5-DMB-Cer using a series of lipid vesicles containing POPC and various amounts of C_5-DMB-Cer as calibration standards. The final concentration of C_5-DMB-Cer was 0.125 mM in each sample. Bar, 10 μm.

and (*c*) the BODIPY fluorophore is less polar than NBD, and, as a result, BODIPY-labeled lipid analogues may be better intercalated in the membrane bilayer. All of the BODIPY Cer analogues accumulated to some extent at the Golgi apparatus of cells in a manner similar to C_6-NBD-Cer, suggesting that this phenomenon is a general property of the Cer molecule, rather than the attached NBD or BODIPY fluorophores, which differ structurally.

Concentration of BODIPY Cer Analogues in Membranes Results in Altered Spectral Properties

A novel feature of C_5-DMB-Cer was that its spectral properties changed with concentration in membranes. This property allowed us to "visually isolate" the Golgi apparatus from other C_5-DMB–labeled intracellular membranes, and represents a considerable improvement over C_6-NBD-Cer for

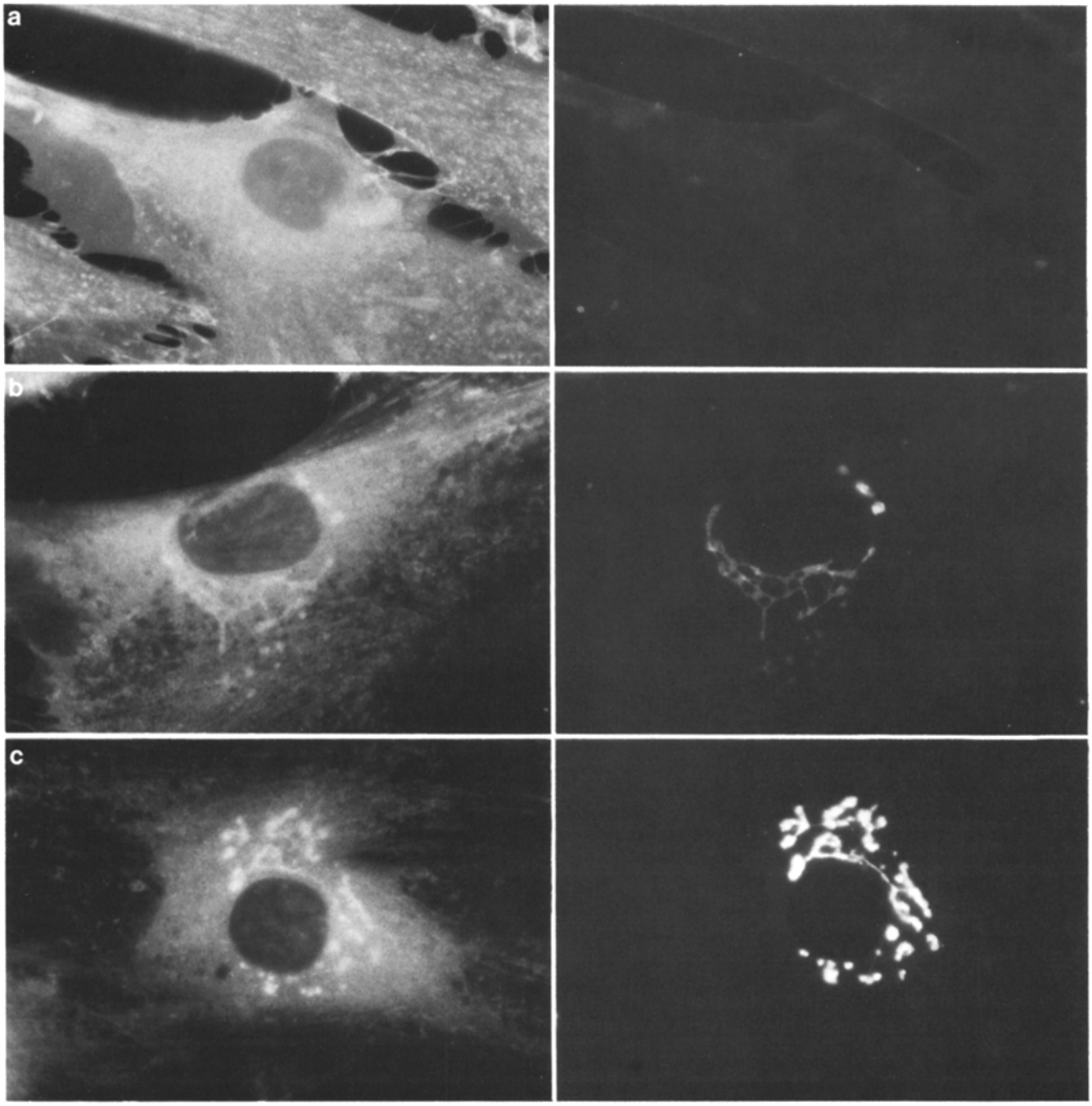

Figure 6. Distribution of C_5-DMB-Cer and its metabolites in cells with time at 37°C. Human skin fibroblasts were incubated with 5 μM C_5-DMB-Cer/DF-BSA for 30 min at 2°C, washed, further incubated in HMEMB for (*a*) 0, (*b*) 5, (*c*) 15, (*d*) 30, (*e*) 60, or (*f*) 120 min at 37°C, and photographed in the green + red (*left*) and red (*right*) microscope channels. Note the presence (at *arrows*) of small fluorescent "spots" in the red channel micrographs in (*d–f*). For a given microscope channel, all photomicrographs were exposed and printed identically. Bar, 20 μm.

vital staining of the Golgi apparatus of various cell types (Fig. 9). In addition, this feature allowed us to visualize fine tubulovesicular processes extending from the Golgi apparatus (Fig. 7 *c*) which were not readily detected in C_6-NBD-Cer–treated cells, presumably because of interfering fluorescence from other regions of the cell, or because the NBD fluorophore bleached too rapidly.

Based on our studies with model membranes, the spectral shift in C_5-DMB-fluorescence at the Golgi apparatus suggests that C_5-DMB-Cer and its metabolites were present at this organelle in higher concentrations than in other regions of the cell. From fluorescence ratio imaging microscopy (Fig. 5), we estimate an upper limit for that concentration of ~5–10 mol %. However, it is not known whether C_5-

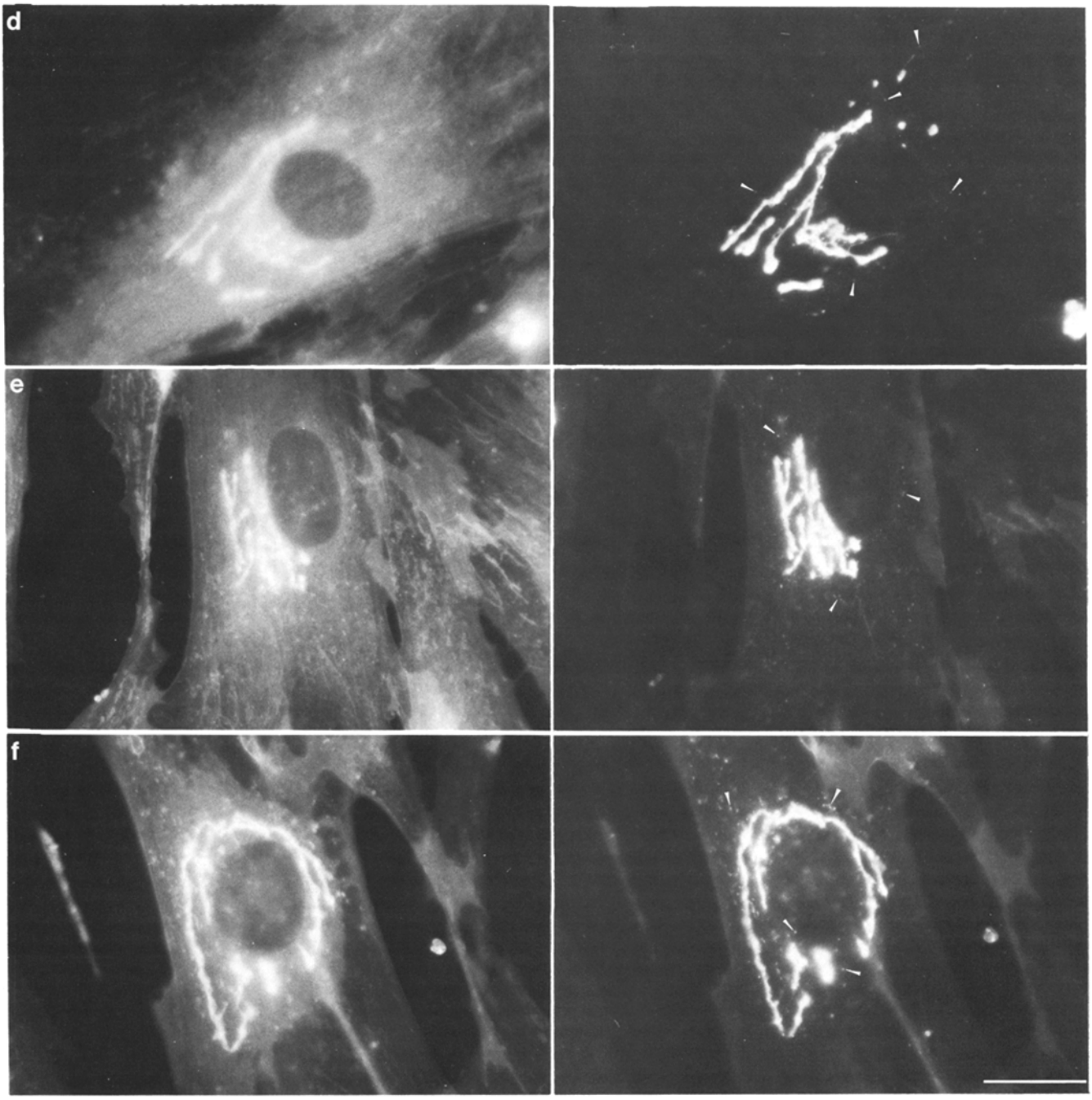

Figure 6.

DMB-Cer and its metabolites were randomly distributed in the membranes of the Golgi apparatus or segregated within "microdomains" (13, 15, 16, 46) which were enriched with these lipids. Such segregation would lead to an apparent high concentration of C_5-DMB-lipids in our measurements, while the actual concentration was much lower. Finally, we emphasize that the molar density of C_5-DMB-lipids obtained in the present study can only be considered approximate since (*a*) the standard curve relating the fluorescence ratio to molar density was obtained in liposomes which are very different in composition from the membranes of the Golgi apparatus; and (*b*) we have not fully evaluated potential polarization artifacts resulting from orientation of the probe in the specimen and polarization of the exciting light in the fluorescence microscope (1, 10).

Intracellular Transport of C_5-DMB-Lipids and Metabolism of C_5-DMB-Cer

We demonstrated that the concentration-dependent spectral properties of C_5-DMB-lipids could be used to monitor the

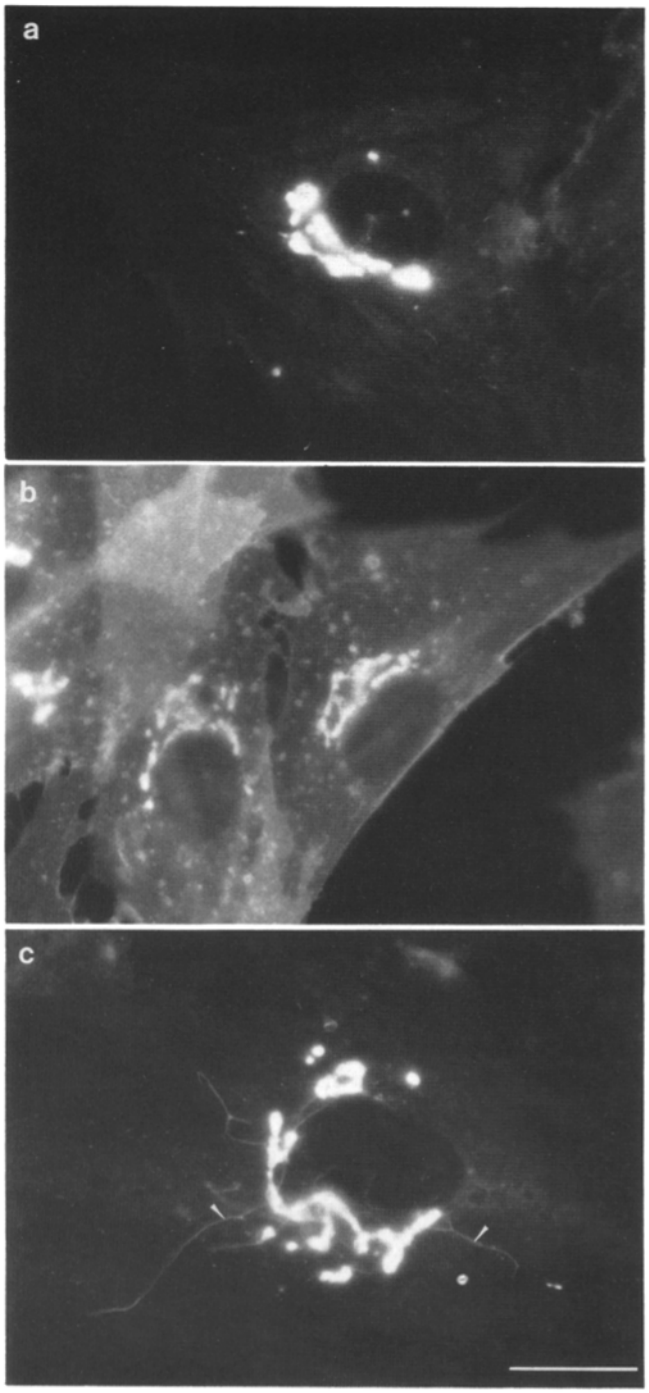

Figure 7. Effect of temperature on the distribution of C_5-DMB-Cer at the Golgi apparatus of human skin fibroblasts. Cells were incubated with 5 μM C_5-DMB-Cer/DF-BSA for 30 min at 2°C, washed, warmed to 37°C for 30 min, and then further incubated in HMEMB for (*a*) 120 min at 20°C, (*b*) 90 min at 37°C, or (*c*) 60 min at 22°C, and photographed in the red microscope channel. Note the absence of plasma membrane labeling in *a*, and the presence of spike-like projections from the Golgi apparatus at arrows in *c*. In *a* and *b*, the plane of focus was at the plasma membrane; both micrographs were exposed and printed identically. Bar, 20 μm.

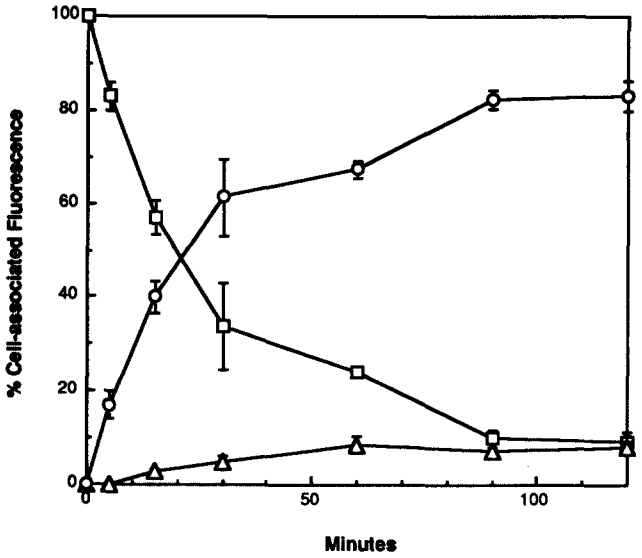

Figure 8. Metabolism of C_5-DMB-Cer in cells with time. Human skin fibroblasts were incubated with 5 μM C_5-DMB-Cer/DF-BSA for 30 min at 2°C, washed, and further incubated in HMEMB at 37°C for the indicated times. Cellular lipids were then extracted and analyzed by TLC using $CHCl_3/CH_3OH$/15 mM $CaCl_2$ as the solvent system. R_f values for C_5-DMB-Cer, -SM, and -GlcCer were 0.85, 0.26, and 0.64, respectively. Data points correspond to C_5-DMB-Cer (□—□), -SM (○—○), and -GlcCer (△—△) and are the means ± SD of three determinations. Cells contained 5.42 ± 0.46 pmol C_5-DMB-Cer/μg protein (n = 3) after the 2°C labeling.

delivery of fluorescent lipid from the Golgi complex to the cell surface. Thus, at early times after incubation with C_5-DMB-Cer, only the Golgi apparatus was visibly fluorescent, but later the plasma membrane became fluorescent and increased in intensity (Fig. 6, red channel). Consistent with the delivery of fluorescent lipids from the Golgi complex to the plasma membrane, we also detected numerous small "spots" of fluorescence in the cytoplasm prior to the appearance of fluorescence at the plasma membrane. Since these structures emitted red fluorescence, we assume that they contained high concentrations of C_5-DMB-lipids, and we speculate that they were transport vesicles which were derived from the Golgi apparatus and were en route to the plasma membrane. Such vesicles would be consistent with the numerous DAB-positive, Golgi apparatus–associated vesicles seen in electron micrographs of C_5-DMB-Cer–treated cells (Fig. 4). Finally, we note that the appearance of fluorescence at the plasma membrane was inhibited when cells were incubated at 20°C, rather than 37°C (Fig. 7, *a* and *b*). This result further suggests that delivery of fluorescent lipids to the cell surface was by a vesicle-mediated process since incubation at low temperatures blocks vesicle transport along the secretory pathway (37, 40).

Although C_5-DMB-Cer was significantly metabolized to C_5-DMB-SM, only a small amount of the corresponding GlcCer analogue was formed (Fig. 8). This is in contrast to

Figure 9. Comparison of C_5-DMB-Cer and C_6-NBD-Cer labeling of various cell types. Cells were incubated with 5 μM C_5-DMB-Cer (or C_6-NBD-Cer)/DF-BSA for 30 min at 2°C, washed, and further incubated in HMEMB for 30 min at 37°C before observation and photography. (*a*) Human skin fibroblasts; (*b*) Swiss 3T3 fibroblasts; (*c*) BHK fibroblasts; (*d*) chicken skeletal muscle cells. (*left panels*) C_6-NBD-, green channel; (*right panels*) C_5-DMB-, red channel. Bar, 20 μm.

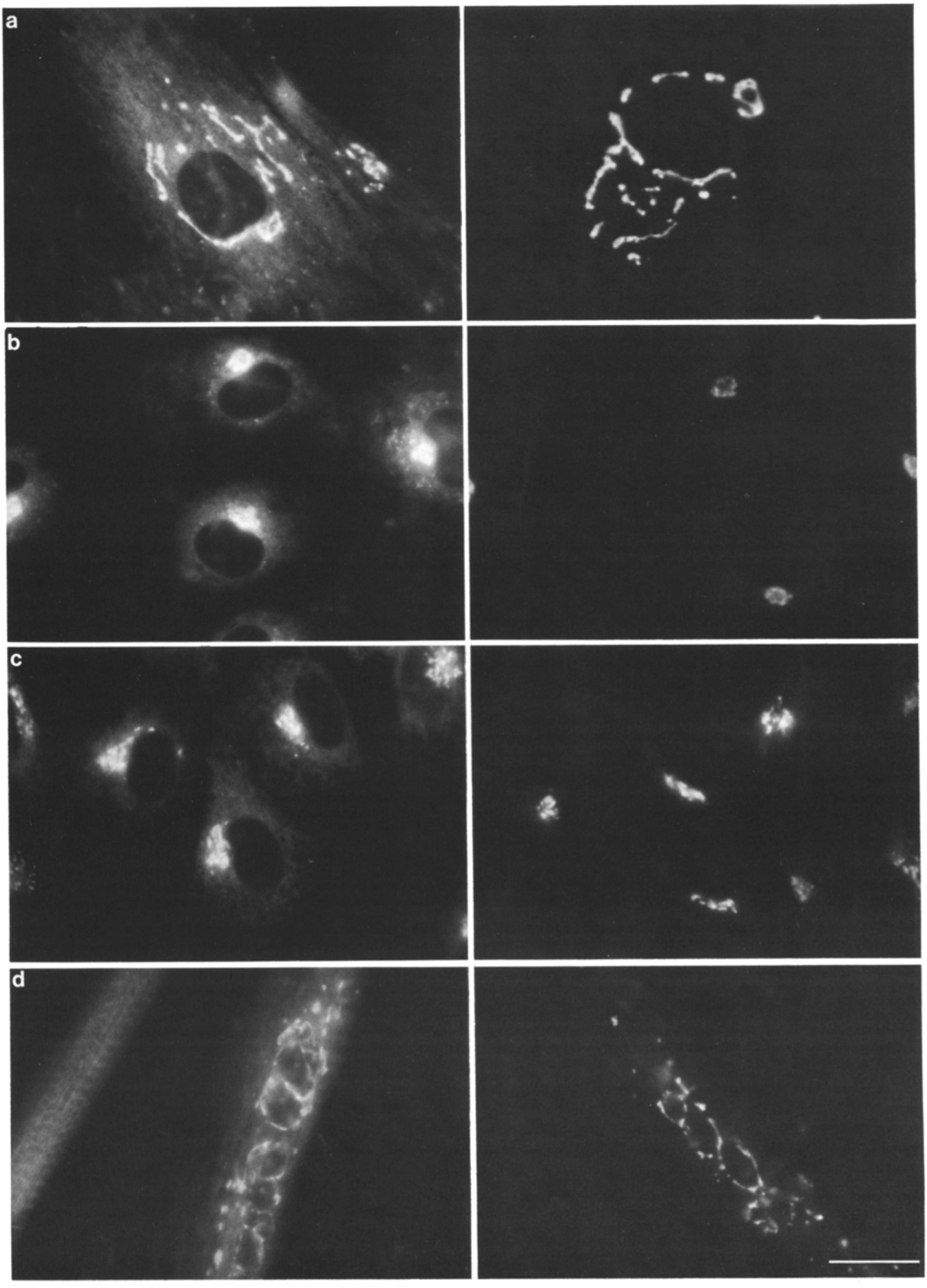
a
b
c
d

the metabolism of C_6-NBD-Cer in human skin fibroblasts where the ratio of de novo synthesized C_6-NBD-SM to -GlcCer is ~1.3/1 under similar incubation conditions (19). The reason for this difference is unknown. One possibility is that the BODIPY fluorophore inhibits the enzyme involved in GlcGer synthesis. However, in preliminary studies we found no inhibition of GlcCer synthesis when *N*-(1-[^{14}C]-hexanoyl)-D-*erythro*-sphingosine (11) was used as a substrate in cultured cells in the presence of C_5-DMB-Cer (R. E. Pagano, unpublished observations). Another possibility is that only small amounts of C_5-DMB-Cer reach the intracellular compartment(s) where the majority of GlcCer synthesis occurs. Indeed, unlike SM synthesis, which is principally restricted to the Golgi apparatus (11, 14), recent studies suggest that significant amounts of GlcCer may be synthesized in a pre- or early Golgi apparatus compartment (42; Futerman, A. H., and R. E. Pagano, manuscript submitted for publication). Finally, it is possible that C_5-DMB-Cer is a poor substrate for GlcCer synthase because of the nature of the BODIPY fatty acid. This explanation is consistent with recent studies by Stein et al. (39), in which it was shown that the metabolic fate of ceramides is critically dependent upon the acyl chain composition of the sphingolipid precursor.

In previous studies using C_6-NBD-lipids, it has been possible to quantify the transport of the fluorescent metabolites to the plasma membrane by measuring the amount and type of NBD lipid that can be removed from the cell surface by incubation with BSA (44, 45) or with nonfluorescent liposomes (17, 18, 19, 23, 25) ("back-exchange"). This approach is possible because most C_6-NBD-lipids exhibit high rates of spontaneous monomeric transfer between membranes in vitro (27, 28, 29, 34). In contrast, we have not been able to deplete C_5-DMB-lipids from the cell surface using a variety of back-exchange conditions, suggesting that spontaneous transfer of these lipids from the plasma membrane to an appropriate acceptor is a much slower process. While this is an apparent limitation of C_5-DMB-Cer, it should be possible to take advantage of the concentration-dependent spectral properties of C_5-DMB-lipids to quantify their intracellular transport. In addition, when this methodology is extended to other fluorescent lipids and their precursors (34), the concentration-dependent spectral properties of the BODIPY fluorophore may yield important new information about the metabolism and intracellular distribution of other lipids (reviewed in 31, 43) within living cells.

The authors thank Dr. D. Fambrough for the chicken skeletal muscle cultures; Mr. J. Bai and Mr. M. Sepanski for technical assistance; and Drs. L. Brand, D. Wolf, and A. Ting for helpful suggestions. We also thank Drs. A. G. Rosenwald and K. J. Longmuir for critical reading of the manuscript.

This work was supported by U. S. Public Health Service grants R37 GM-22942 and GM-37434 to R. E. Pagano, and National Institutes of Health Small Business Innovation Research grant GM-37347 to R. P. Haugland.

Received for publication 28 December 1990 and in revised form 23 February 1991.

References

1. Axelrod, D. 1979. Carbocyanine dye orientation in red cell membranes studied by microscopic fluorescence polarization. *Biophys. J.* 26:557–574.
2. Bergeron, J. J. M., R. A. Rachubinski, R. A. Sikstrom, B. I. Posner, and J. Paiement. 1982. Galactose transfer to endogenous acceptors within Golgi fractions of rat liver. *J. Cell Biol.* 92:139–146.
3. Bligh, E. G., and W. J. Dyer. 1959. A rapid method of total lipid extraction and purification. *Can. J. Biochem. Physiol.* 37:911–917.
4. Bright, G. R., G. W. Fisher, J. Rogowska, and D. L. Taylor. 1987. Fluorescence ratio imaging microscopy: temporal and spatial measurements of cytoplasmic pH. *J. Cell Biol.* 104:1019–1033.
5. Bright, G. R., G. W. Fisher, J. Rogowska, and D. L. Taylor. 1989. Fluorescence ratio imaging microscopy. *In* Methods in Cell Biology: Fluorescence Microscopy of Living Cells in Culture. Vol. 30, part B. D. L. Taylor and Y.-L. Wang, editors. Academic Press, New York. 157–192.
6. Chattopadhyay, A. 1990. Chemistry and biology of *N*-(7-nitrobenz-2-oxa-1,3-diazol-4-yl)-labeled lipids: fluorescent probes of biological and model membranes. *Chem. Phys. Lipids.* 53:1–15.
7. Chattopadhyay, A., and E. London. 1987. Parallax method for direct measurement of membrane penetration depth utilizing fluorescence quenching by spin-labeled phospholipids. *Biochemistry.* 26:39–45.
8. Cooper, M. S., A. H. Cornell-Bell, A. Chernjavsky, J. W. Dani, and S. J. Smith. 1990. Tubulovesicular processes emerge from *trans*-Golgi cisternae, extend along microtubules, and interlink adjacent *trans*-Golgi elements into a reticulum. *Cell.* 61:135–145.
9. Devreotes, P. N., and D. M. Fambrough. 1975. Acetylcholine receptor turnover in membranes of developing muscle fibers. *J. Cell Biol.* 65: 335–358.
10. Dragsten, P. R., and W. W. Webb. 1978. Mechanism of the membrane potential sensitivity of the fluorescent membrane probe Merocyanine 540. *Biochemistry.* 17:5228–5240.
11. Futerman, A. H., B. Stieger, A. L. Hubbard, and R. E. Pagano. 1990. Sphingomyelin synthesis in rat liver occurs predominantly at the *cis* and *medial* cisternae of the Golgi apparatus. *J. Biol. Chem.* 265:8650–8657.
12. Hope, M. J., M. B. Bally, G. Webb, and P. R. Cullis. 1985. Production of large unilamellar vesicles by a rapid extrusion procedure. Characterization of size distribution, trapped volume and ability to maintain a membrane potential. *Biochim. Biophys. Acta.* 812:55–65.
13. Jain, M. K. 1983. Nonrandom lateral organization in bilayers and biomembranes. *In* Membrane Fluidity in Biology. Vol. 1. R. C. Aloia, editor. Academic Press, New York. 1–37.
14. Jeckel, D., A. Karrenbauer, R. Birk, R. R. Schmidt, and F. Wieland. 1990. Sphingomyelin is synthesized in the *cis* Golgi. *FEBS (Fed. Eur. Biochem. Soc.) Lett.* 261:155–157.
15. Karnovsky, M. J., A. M. Kleinfeld, R. L. Hoover, and R. D. Klausner. 1982. The concept of lipid domains in membranes. *J. Cell Biol.* 94:1–6.
16. Klausner, R. D., and D. E. Wolf. 1990. Selectivity of fluorescent lipid analogues for lipid domains. *Biochemistry.* 19:6199–6203.
17. Kobayashi, T., and R. E. Pagano. 1989. Lipid transport during mitosis: alternative pathways for delivery of newly synthesized lipids to the cell surface. *J. Biol. Chem.* 264:5966–5973.
18. Koval, M., and R. E. Pagano. 1989. Lipid recycling between the plasma membrane and intracellular compartments: transport and metabolism of fluorescent sphingomyelin analogs in cultured fibroblasts. *J. Cell Biol.* 108:2169–2181.
19. Koval, M., and R. E. Pagano. 1990. Sorting of an internalized plasma membrane lipid between recycling and degradative pathways in normal and Niemann-Pick, type A fibroblasts. *J. Cell Biol.* 111:429–442.
20. Kremer, J. M. H., M. W. J. v. d. Esker, C. Pathmamanoharan, and P. H. Wiersema. 1977. Vesicles of variable diameter prepared by a modified injection method. *Biochemistry.* 16:3932–3935.
21. Lippincott-Schwartz, J., J. G. Donaldson, A. Schweizer, E. G. Berger, H. P. Hauri, L. C. Yuan, and R. D. Klausner. 1990. Microtubule-dependent retrograde transport of proteins into the ER in the presence of Brefeldin A suggests an ER recycling pathway. *Cell.* 60:821–836.
22. Lipsky, N. G., and R. E. Pagano. 1983. Sphingolipid metabolism in cultured fibroblasts: microscopic and biochemical studies employing a fluorescent ceramide analogue. *Proc. Natl. Acad. Sci. USA.* 80:2608–2612.
23. Lipsky, N. G., and R. E. Pagano. 1985. Intracellular translocation of fluorescent sphingolipids in cultured fibroblasts: endogenously synthesized sphingomyelin and glucosylcerebroside analogues pass through the Golgi apparatus en route to the plasma membrane. *J. Cell Biol.* 100:27–34.
24. Lipsky, N. G., and R. E. Pagano. 1985. A vital stain for the Golgi apparatus. *Science (Wash. DC).* 228:745–747.
25. Martin, O. C., and R. E. Pagano. 1987. Transbilayer movement of fluorescent analogs of phosphatidylserine and phosphatidylethanolamine at the plasma membrane of cultured cells. *J. Biol. Chem.* 262:5890–5898.
26. Moranto, A. R. 1982. Neuronal mapping: a photooxidation reaction makes Lucifer Yellow useful for electron microscopy. *Science (Wash. DC).* 217:953–955.
27. Nichols, J. W., and R. E. Pagano. 1981. Kinetics of soluble lipid monomer diffusion between vesicles. *Biochemistry.* 20:2783–2789.
28. Nichols, J. W., and R. E. Pagano. 1982. Use of resonance energy transfer to study the kinetics of amphiphile transfer between vesicles. *Biochemistry.* 21:1720–1726.
29. Pagano, R. E. 1989. A fluorescent derivative of ceramide: physical properties and use in studying the Golgi apparatus of animals cells. *In* Methods in Cell Biology: Fluorescence Microscopy of Living Cells in Culture. Vol. 29, part A. D. L. Taylor and Y.-L. Wang, editors. Academic Press, New York. 75–85.

30. Pagano, R. E. 1990. The Golgi apparatus: insights from lipid biochemistry. *Biochem. Soc. Trans.* 18:361–366.
31. Pagano, R. E. 1990. Lipid traffic in eukaryotic cells: mechanisms for intracellular transport and organelle-specific enrichment of lipids. *Curr. Opin. Cell Biol.* 2:652–663.
32. Pagano, R. E., and O. C. Martin. 1988. A series of fluorescent *N*-(acyl)-sphingosines: synthesis, physical properties, and studies in cultured cells. *Biochemistry.* 27:4439–4445.
33. Pagano, R. E., M. A. Sepanski, and O. C. Martin. 1989. Molecular trapping of a fluorescent ceramide analogue at the Golgi apparatus of fixed cells: interaction with endogenous lipids provides a *trans*-Golgi marker for both light and electron microscopy. *J. Cell Biol.* 109:2067–2079.
34. Pagano, R. E., and R. G. Sleight. 1985. Defining lipid transport pathways in animal cells. *Science (Wash. DC).* 229:1051–1057.
35. Rouser, B., A. N. Siakotos, and S. Fleischer. 1981. Quantitative analysis of phospholipids by thin-layer chromatography and phosphorous analysis of spots. *Lipids.* 1:85–86.
36. Sandell, J. H., and R. Masland. 1988. Photoconversion of some fluorescent markers to a diaminobenzidine product. *J. Histochem. Cytochem.* 36: 555–559.
37. Saraste, J., G. E. Palade, and M. G. Farquhar. 1986. Temperature-sensitive steps in the transport of secretory proteins through the Golgi complex in exocrine pancreatic cells. *Proc. Natl. Acad. Sci. USA.* 83:6425–6429.
38. Schwarzmann, G., and K. Sandhoff. 1987. Lysogangliosides: synthesis and use in preparing labeled gangliosides. *Methods Enzymol.* 138:319–341.
39. Stein, O., K. Oette, G. Hollander, Y. Dabach, M. Ben-Naim, and Y. Stein. 1989. Divergent fate of unsaturated and saturated ceramides and sphingomyelins in rat liver and cells in culture. *Biochim. Biophys. Acta.* 1003:175–182.
40. Tartakoff, A. 1986. Temperature and energy dependence of secretory protein transport in the exocrine pancreas. *EMBO (Eur. Mol. Biol. Organ.) J.* 5:1477–1482.
41. Ting, A. E., and R. E. Pagano. 1990. Detection of a phosphatidyl-inositol-specific phospholipase C at the surface of Swiss 3T3 cells and its potential role in the regulation of cell growth. *J. Biol. Chem.* 265:5337–5340.
42. van Echten, G., and K. Sandhoff. 1989. Modulation of ganglioside biosynthesis in primary cultured neurons. *J. Neurochem.* 52:207–214.
43. van Meer, G. 1989. Lipid traffic in animal cells. *Annu. Rev. Cell Biol.* 5:247–275.
44. van Meer, G., E. H. K. Stelzer, W. Wijnaendts-van-Resandt, and K. Simons. 1987. Sorting of sphingolipids in epithelial (Madin-Darby canine kidney) cells. *J. Cell Biol.* 105:1623–1635.
45. van't Hof, W., and G. van Meer. 1990. Generation of lipid polarity in intestinal epithelial (Caco-2) cells: sphingolipid synthesis in the Golgi complex and sorting before vesicular traffic to the plasma membrane. *J. Cell Biol.* 111:977–986.
46. Yechiel, E., and M. Edidin. 1987. Micrometer-scale domains in fibroblast plasma membranes. *J. Cell Biol.* 105:755–760.